

FORWARD JETS, DIJETS, AND SUBJETS AT THE TEVATRON

LEVAN BABUKHADIA

Physics Department, University of Arizona, Tucson, AZ 85721, USA

on behalf of the CDF and DØ Collaborations

Recent new results on the determination of the rapidity dependence of the differential inclusive jet cross section, $\langle d^2\sigma/dE_T d\eta \rangle$, as a function of jet E_T in $p\bar{p}$ collisions at $\sqrt{s} = 1800$ GeV, measured by the DØ detector at the Tevatron, are presented along with the comparisons to theoretical next-to-leading order (NLO) perturbative QCD predictions. Triple differential dijet cross sections, $\langle d^3\sigma/dE_T d\eta_1 d\eta_2 \rangle$, at $\sqrt{s} = 1800$ GeV, as well as the new results on jet structure at $\sqrt{s} = 1800$ and 630 GeV, as measured by the CDF and DØ detectors, are also discussed.

1 Introduction

The last decade of the 20th century in high energy physics will undoubtedly be noted for the impressive progress made in both theoretical and experimental understanding of collimated streams of particles or “jets” resulting from inelastic hadron collisions. The Fermilab Tevatron $p\bar{p}$ Collider, having operated at center-of-mass (CM) energies of 1800 GeV and 630 GeV, is a prominent arena for experimentally studying hadronic jets. Theoretically, jet production in $p\bar{p}$ collisions is understood within the framework of quantum chromodynamics (QCD) as a hard scattering of the constituents of protons, quarks and gluons (or partons) that, having undergone the collision, manifest themselves as jets in the final state. Studying various jet properties in the two collider experiments, CDF and DØ, therefore provides stringent tests of QCD. In what follows, we discuss recent results from the two experiments, spanning topics from the short to long range physics of jets.

2 Tests of pQCD — Jet Cross Sections

Perturbative QCD (pQCD) theoretical calculations of various jet cross sections¹ and new, accurately determined parton distribution functions (pdf’s)² add particular interest to the corresponding experimental cross section measurements at the Tevatron. These measurements test the short range behavior of QCD, the structure of proton in terms of pdf’s, and, if it exists, the substructure of quarks and gluons. The cross section measurements reported here are based on integrated luminosities of 87 and 92 pb⁻¹ collected by the CDF

and DØ experiments, respectively, during the 1994–95 Tevatron run.

In both experiments, jets are reconstructed using an iterative cone algorithm with a fixed cone radius of $\mathcal{R} = 0.7$ in $\eta - \varphi$ space, where pseudorapidity η is related to the polar angle (from the beam line) θ via $\eta = \ln[\cot \theta/2]$ and φ is the azimuthal angle. The offline data selection procedure eliminates contamination from background events caused by electrons, photons, noise, or cosmic rays. This is achieved by applying an acceptance cut on the z -coordinate of the interaction vertex, flagging events with large missing transverse energy, and applying jet quality cuts. Details of data selection and corrections due to noise and/or contamination are described elsewhere ³.

Furthermore, the jet energy scale correction removes instrumentation effects associated with calorimeter response, showering, and noise, as well as the contribution from spectator partons. The energy scale corrects jets from their reconstructed E_T to their “true” E_T , on average. The smearing effects of the finite calorimeter resolutions on jet cross sections are removed by an unfolding procedure. In DØ, the scale and resolution corrections are determined mostly from the data and are applied in two separate steps, while in CDF both corrections are done in a single step by means of a Monte Carlo (MC) tuned to the data.

2.1 Rapidity Dependence of the Inclusive Jet Cross Section

Recently, DØ has made a new measurement of the rapidity dependence of the inclusive single jet cross section. The cross section is determined as a function of jet transverse energy E_T in five intervals of jet $|\eta|$, up to $|\eta| = 3.0$, significantly extending previously available inclusive jet cross section measurements up to $|\eta| = 0.7$. The single inclusive jet cross section is calculated from the number of jets in each $\eta - E_T$ bin, scaled by the integrated luminosity, data selection inefficiencies, and the unfolding correction. The experimental measurement in each of the five $|\eta|$ regions is compared to the α_s^3 theoretical predictions by JETRAD (Giele, *et al.* ¹) with renormalization and factorization scales set equal to each other and to $E_T^{max}/2$ and the parton clustering parameter $R_{sep} = 1.3$. Comparisons have been made to all recent pdf’s of the CTEQ and MRST families ⁴. Fig. 1 shows the comparisons with the CTEQ3M pdf on a linear scale. The error bars are statistical uncertainties, while the error bands indicate 1σ systematic uncertainties. Theoretical uncertainties are on the order of the systematic errors. The jet cross section, which spans seven orders of magnitude from the lowest to the highest E_T ’s considered, agrees within errors with the theoretical pQCD predictions over the full dynamical range.

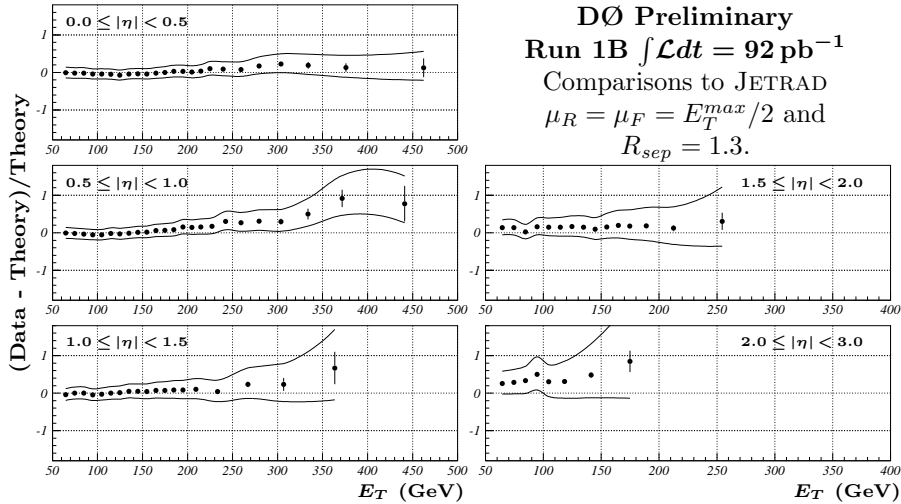


Figure 1. The comparisons between the DØ single inclusive jet production cross section, $\langle d^2\sigma/dE_T d\eta \rangle$, as a function of jet E_T in five jet η regions (up to $|\eta| = 3.0$) and the α_s^3 QCD predictions calculated by JETRAD with the CTEQ3M pdf.

2.2 Triple Differential Dijet Cross Section

CDF and DØ have measured the triple differential dijet cross sections, which are generally less sensitive to the pQCD matrix elements and more sensitive to the pdf's. In CDF, the trigger jet has $E_T > 40$ GeV and is central ($|\eta| < 0.7$), while the probe jet has $E_T > 10$ GeV and sweeps all four $|\eta|$ regions considered (up to $|\eta| = 3.0$). Fig. 2 shows the comparisons of the CDF measurement to the α_s^3 pQCD predictions obtained by JETRAD with three different pdf's and input parameter values as indicated. The systematic uncertainties are highly correlated. The data tend to be higher than pQCD at large E_T 's. CTEQ4HJ pdf shows better agreement with the data at high E_T 's. Theoretical uncertainties are about as large as the systematics errors.

In DØ, the E_T 's of *both* jets are measured, even at highest η 's, so as to be able to also reconstruct Bjorken x values for the hard scattered partons. The data are divided into four $|\eta|$ regions which are further split into Same Side (SS), $\eta_1 \cdot \eta_2 > 0$, and Opposite Side (OS), $\eta_1 \cdot \eta_2 < 0$, dijet events and thus a total of eight cross sections are measured (up to $|\eta| = 2.0$). Since E_T 's of both jets are determined, there are two entries per event in each of the eight cross sections. The comparisons with JETRAD predictions are shown in Fig. 3, where statistical errors are indicated by the error bars, and the upper and lower sets of symbols define the 1σ systematic error band.

CDF Preliminary

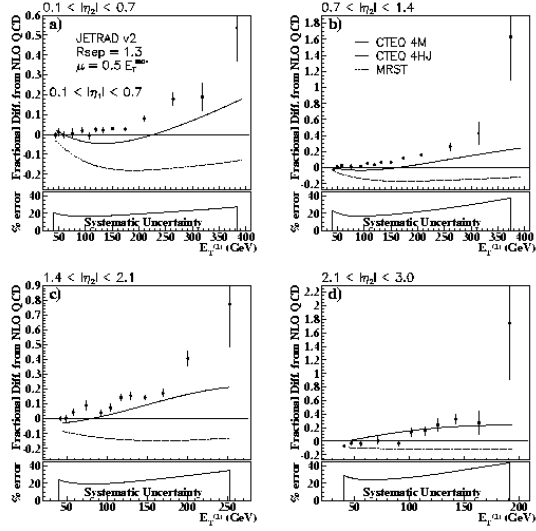


Figure 2. Comparisons of the CDF triple differential dijet cross sections to α_s^3 QCD JETRAD theoretical calculations with various pdf's, normalized to the predictions with CTEQ4M pdf. Note different y -scales of the plots corresponding to different $|\eta|$ regions ($|\eta| < 3.0$). Systematic errors are shown in percent at the bottom of each plot.

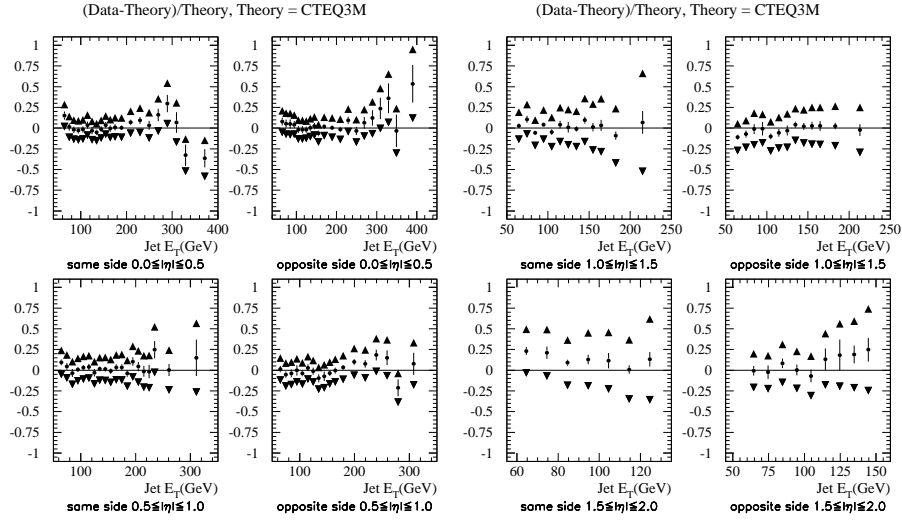


Figure 3. The comparison between the $D\bar{O}$ dijet triple differential jet cross section as a function of jet E_T in four jet η regions (up to $|\eta| = 2.0$) for the SS and OS topologies, and the α_s^3 QCD predictions calculated by JETRAD with the CTEQ3M pdf.

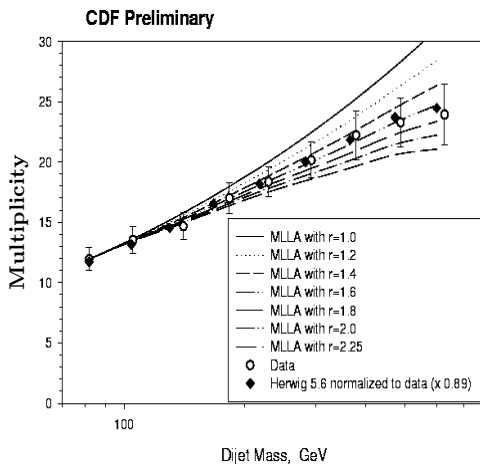


Figure 4. Charged multiplicity within a fixed opening angle of 0.466 rad around the jet axis in dijets. The data are compared to the HERWIG MC as well as to the MLLA/LPHD predictions with $r = 1.0$ – 2.25 . A model dependent value of $r = 1.7 \pm 0.3$ is extracted.

3 Tests of the Large Scale QCD — Jet Structure

While jet cross sections are described by the pQCD and pdf's, the structure of a jet is determined by the large scale QCD behavior which requires non-perturbative methods for calculations. In naive QCD, the ratio r of multiplicities in gluon and quark jets is expected to be proportional to the ratio of their color charges: $r = C_A/C_F = 9/4$. In the framework of the Modified Leading Logarithmic Approximation (MLLA)⁵ with the assumption of Local Parton–Hadron Duality (LPHD)⁶, the ratio r is expected to decrease with the inclusion of NLO and next-to-next-to-leading (NNLO) order terms. CDF has measured the charged track multiplicity in dijets presented in Fig. 4 as a function of the dijet mass along with the HERWIG MC and MLLA/LPHD calculations, the latter with various values of the input parameter r . The best fit to the MLLA/LPHD predictions yields a model dependent value of $r = 1.7 \pm 0.3$. CDF has also measured inclusive momentum distributions of charged particles in dijets and thereby has obtained the MLLA/LPHD free parameter $Q_{\text{eff}} (\sim \Lambda_{\text{QCD}}) = 240 \pm 40$ MeV.

DØ has measured the gluon and quark subjet multiplicities (M_g and M_q , respectively) by means of a successive combination k_T jet algorithm⁷. In order to not bias the measurement by gluon/quark jet tagging criteria, similar samples are compared at $\sqrt{s} = 1800$ and 630 GeV in the same jet E_T (55–100 GeV) and η intervals ($|\eta| < 0.5$). The HERWIG MC predictions of the fraction of the gluon jets at the two CM energies of 59 and 33%, respectively, are used to extract the subjet multiplicities in gluon and quark jets shown in Fig. 5.

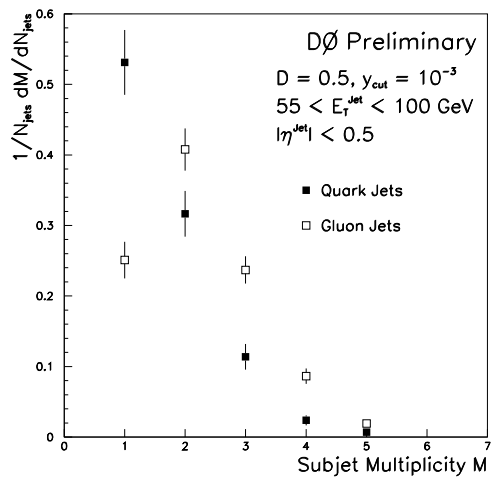


Figure 5. Subjet multiplicities in quark and gluon jets extracted from $D\bar{0}$ data indicating that, on average, gluon jets have more subjet clusters than quark jets. The k_T algorithm is used for jet and subjet reconstruction with a “resolution” parameter $y_{\text{cut}} = 10^{-3}$ and the “distance” scale parameter of the jet algorithm in $\eta - \varphi$ space of $D = 0.5$.

Furthermore, the ratio of gluon to quark subjet multiplicities is measured at $r \equiv (\langle M_g \rangle - 1) / (\langle M_q \rangle - 1) = 1.91 \pm 0.04(\text{stat})_{-0.19}^{+0.23}(\text{sys})$.

In conclusion, CDF and $D\bar{0}$ experiments have made several measurements to test the short as well as the long range behavior of QCD. Measurements are in good agreement with theoretical predictions.

References

1. W.T. Giele, E.W.N. Glover, and D.A. Kosower, Phys. Rev. Lett. **73**, 2019 (1994); S.D. Ellis, Z. Kunszt, and D.E. Soper, Phys. Rev. Lett. **64**, 2121 (1990); F. Aversa *et al.*, Phys. Rev. Lett. **65**, (1990).
2. H.L. Lai *et al.*, (CTEQ Collaboration) Phys. Rev. **D51**, 4763 (1995); A.D. Martin *et al.*, (MRST Collaboration) Eur. Phys. J. **C4**, 463 (1998).
3. F. Abe *et al.*, (CDF Collaboration), Phys. Rev. Lett. **77**, 438 (1996); B. Abbott *et al.*, ($D\bar{0}$ Collaboration), Phys. Rev. Lett. **82**, 2451, (1999).
4. L. Babukhadia, http://www-d0.fnal.gov/~blevan/talk_jsmd99/index.htm.
5. Yu. Dokshitzer, S. Troyan, XIX Winter School of LNPI, vol. 1, 144; A. Mueller, Nucl. Phys. **B213** (1983); erratum quoted *ibid.*, **B241** 141 (1984).
6. Yu.I. Azimov, Yu. Dokshitzer, V. Khoze, and S. Troyan, Z. Phys. **C27** 65 (1985) and **C31** 213 (1986).
7. S. Catani, Yu.L. Dokshitzer, M.H. Seymour and B.R. Webber, Nucl.

Phys. **B406** 187 (1993). S.D. Ellis and D.E. Soper, Phys. Rev. **D48**
3160 (1993).